Physics Letters B 736 (2014) 119–123

Contents lists available at ScienceDirect

Physics Letters B

www.elsevier.com/locate/physletb

Ab initio path to heavy nuclei

Sven Binder *, Joachim Langhammer, Angelo Calci, Robert Roth

Institut für Kernphysik, Technische Universität Darmstadt, Schlossgartenstr. 2, 64289 Darmstadt, Germany

ARTICLE INFO

Article history:
Received 24 March 2014
Received in revised form 1 July 2014
Accepted 7 July 2014
Available online 9 July 2014
Editor: J.-P. Blaizot

Keywords:
Ab initio nuclear structure theory
Chiral effective field theory
Coupled-cluster theory
Heavy nuclei

ABSTRACT

We present the first *ab initio* calculations of nuclear ground states up into the domain of heavy nuclei, spanning the range from ^{16}O to ^{132}Sn, based on two- plus three-nucleon interactions derived within chiral effective field theory. We employ the similarity renormalization group for preparing the Hamiltonian and use coupled-cluster theory to solve the many-body problem for nuclei with closed sub-shells. Through an analysis of theoretical uncertainties resulting from various truncations in this framework, we identify and eliminate the technical hurdles that previously inhibited the step beyond medium-mass nuclei, allowing for reliable validations of nuclear Hamiltonians in the heavy regime. Following this path we show that chiral Hamiltonians qualitatively reproduce the systematics of nuclear ground-state energies up to the neutron-rich Sn isotopes.

1. Introduction

Hamiltonians derived within chiral effective field theory [1,2] represent a milestone in the endeavor to describe nuclear properties in a universal framework based on QCD. Already at the current stage, chiral two-nucleon (NN) plus three-nucleon ($3N$) Hamiltonians have successfully been applied in a wide range of *ab initio* nuclear structure [3–10] and reaction calculations [11]. Particularly the medium-mass regime has seen amazing progress over the past few years: several *ab initio* many-body methods can nowadays access this regime. The importance-truncated no-core shell model [12,13] provides quasi-exact solutions that serve as benchmark points for computationally efficient medium-mass methods [8]. In addition to its success in quantum chemistry, coupled-cluster theory [4,6] has emerged as one of the most efficient and versatile tools for the accurate computation of (near-)closed-shell nuclei. Alternative approaches are the self-consistent Green's function methods [14–16] and the in-medium similarity renormalization group [8,17,18], which also have been generalized to open-shell systems. While most of the many-body methods above can be applied to heavier systems, challenges regarding the preparation of the Hamiltonian have prevented *ab initio* theory from entering this mass range so far.

In this Letter we overcome these limitations and present *ab initio* calculations of nuclei up to ^{132}Sn using similarity renormalization group (SRG)-transformed chiral $NN + 3N$ interactions. We present key developments in the treatment of the Hamiltonian that enable these calculations, and discuss the remaining uncertainties due to truncations. For the solution of the many-body problem we use coupled-cluster (CC) theory including a non-iterative treatment of triply excited clusters.

2. Preparation of the Hamiltonian

With *ab initio* nuclear structure theory advancing towards heavier systems, the preparation of the $NN + 3N$ Hamiltonian prior to the many-body calculations becomes increasingly important. We start from the chiral NN interaction at N^{3}LO [19] and a local form of the chiral $3N$ interaction at N^{2}LO [20] with regulator cutoff of 400 MeV/c [13,21,22]. To enhance the convergence behavior of the many-body calculations, we soften this initial Hamiltonian through an SRG transformation, formulated as flow equation in terms of a continuous flow parameter α [21,23–25]. The SRG allows to consistently evolve the NN and $3N$ interactions [13] and yields a model-space independent Hamiltonian. One of the challenges is the many-body interactions induced during the SRG flow. For practical reasons we truncate these interactions at the $3N$ level and consequently violate the unitarity of the transformation, which introduces a flow-parameter dependence of observables. This α-dependence carries information about the relevance of omitted many-nucleon interactions and allows conclusions about their origins and importance. We consider two types of Hamiltonians in order to distinguish between the effects of

* Corresponding author.
E-mail addresses: sven.binder@physik.tu-darmstadt.de (S. Binder), joachim.langhammer@physik.tu-darmstadt.de (J. Langhammer), angelo.calci@physik.tu-darmstadt.de (A. Calci), robert.roth@physik.tu-darmstadt.de (R. Roth).

http://dx.doi.org/10.1016/j.physletb.2014.07.010

the initial chiral 3N interaction and SRG-induced contributions: for the $NN+3N$-induced Hamiltonian we start from the chiral NN interaction and keep induced interactions up to the 3N level, whereas for the $NN+3N$-full Hamiltonian we start with the chiral $NN+3N$ interaction and keep all 3N contributions. Due to their enormous number, an energy truncation $e_1+e_2+e_3 \leq E_{3\,\mathrm{max}}$ is imposed on the 3N matrix elements, where the e_i are the principal quantum numbers of the single-particle harmonic-oscillator (HO) basis states. To facilitate our calculations, we mainly use the normal-ordered two-body approximation (NO2B) [22,26] to the 3N interaction, which was proven to be very accurate [22,26,27].

3. Coupled-cluster method

For solving the many-body Schrödinger equation we employ a spherical formulation of CC theory [4,6,28,29], which constitutes a good compromise between accuracy and computational efficiency. In single-reference CC with singles and doubles excitations (CCSD) [30], the ground state $|\Psi\rangle$ of a many-body Hamiltonian is parametrized by the exponential ansatz $|\Psi\rangle = e^{T_1+T_2}|\Phi\rangle$, where T_n are n-particle-n-hole excitation operators acting on a single Slater-determinant reference state $|\Phi\rangle$. Effects of the T_3 clusters are included through an *a posteriori* correction to the energy via the CR-CC(2,3) [31–33] or the ΛCCSD(T) [27,34,35] method. The underlying single-particle basis is an HO basis truncated in the principal oscillator quantum number $2n+l \leq e_{\mathrm{max}}$. We do Hartree–Fock (HF) calculations to optimize the single-particle basis, and perform the normal ordering with respect to the HF ground state.

4. Role of the three-body SRG model space

The SRG evolution is performed in a finite model space and particularly for the evolution of the 3N interaction, the model spaces required to accurately represent the Hamiltonian become very large. We parametrize our SRG model spaces by an angular-momentum dependent truncation $E_{\mathrm{SRG}}(J)$ for the energy quantum numbers in the three-body Jacobi-HO basis in which the flow equation is solved [13,21]. These parametrizations, referred to as *ramps*, are defined by two plateaus of constant $E_{\mathrm{SRG}}(J)$ with a linear slope in between. Earlier works employed ramp $\mathcal{A}$ with $E^{(\mathcal{A})}_{\mathrm{SRG}}(J \leq \frac{5}{2}) = 40$ and $E^{(\mathcal{A})}_{\mathrm{SRG}}(J \geq \frac{13}{2}) = 24$ [8,13,15,18,21,22,27]. Already in medium-mass calculations, this ramp shows first deficiencies [18,36]. If the SRG evolution is performed at small frequencies $\hbar\Omega$, the momentum range covered in the truncated SRG model space is not sufficient to capture the relevant contributions of the initial Hamiltonian, resulting in an artificial increase of the ground-state energies. We overcome this problem using the frequency conversion discussed in [13], where we evolve the Hamiltonian at a sufficiently large frequency $\hbar\Omega_{\mathrm{SRG}}$ and convert to the target frequency subsequently. In Fig. 1 we show the $\hbar\Omega$-dependence of CCSD ground-state energies obtained for ramp $\mathcal{A}$ with and without frequency conversion. This frequency conversion, used in all following calculations, eliminates the artificial increase of the energies at low frequencies and shifts the energy minima towards lower frequencies.

Next we investigate the convergence with respect to the SRG model-space size. To this end, we also employ a considerably larger model space defined by ramp $\mathcal{B}$, with plateaus $E^{(\mathcal{B})}_{\mathrm{SRG}}(J \leq \frac{7}{2}) = 40$ and $E^{(\mathcal{B})}_{\mathrm{SRG}}(J \geq \frac{11}{2}) = 36$. In Fig. 2(a) we compare CCSD ground-state energies obtained for ramps $\mathcal{A}$ and $\mathcal{B}$. For the lighter nuclei both ramps give very similar results, but with increasing mass number we observe an increasing deviation. For ^{56}Ni, this deviation is about 0.4 MeV per nucleon, and grows to around 7 MeV per nucleon for the Sn isotopes. These results dramatically illustrate the

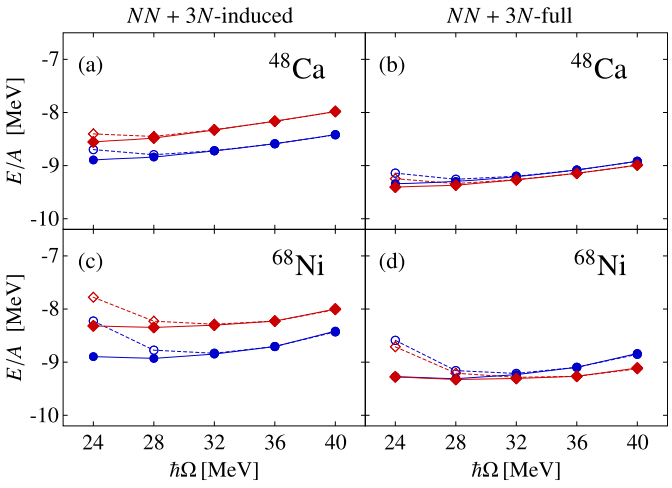

Fig. 1. (Color online.) Comparison of CCSD ground-state energies at flow parameters $\alpha = 0.04$ fm^4 (blue circles) and 0.08 fm^4 (red diamonds), without (open symbols) and with (full symbols) frequency conversion, using $E_{3\,\mathrm{max}} = 14$ and $e_{\mathrm{max}} = 12$. The frequency conversion was performed using the parent frequency $\hbar\Omega_{\mathrm{SRG}} = 36$ MeV.

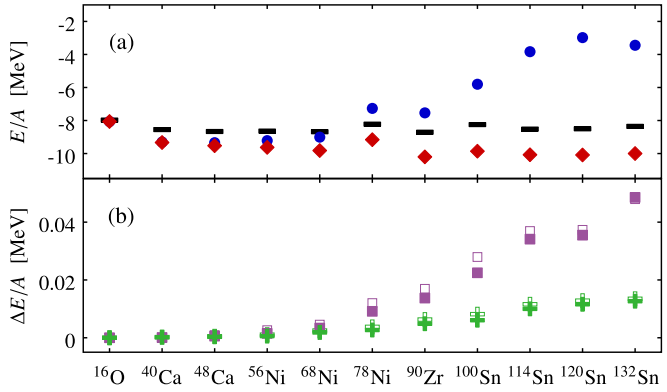

Fig. 2. (Color online.) (a) Comparison of CCSD ground-state energies corresponding to ramp $\mathcal{A}$ (blue circles) and $\mathcal{B}$ (red diamonds) to experiment (black bars) [37]. (b) Deviation of CCSD ground-state energies corresponding to ramp $\mathcal{C}$ (violet boxes) and $\mathcal{D}$ (green crosses) from ramp $\mathcal{B}$ for the $NN+3N$-induced (open symbols) and $NN+3N$-full Hamiltonian (full symbols). All calculations are performed for $E_{3\,\mathrm{max}} = 14$, $\alpha = 0.08$ fm^4, $\hbar\Omega = 24$ MeV and $e_{\mathrm{max}} = 12$.

importance of large SRG model spaces for heavier systems. To assess the truncation errors related to ramp $\mathcal{B}$ we introduce the two auxiliary ramps $\mathcal{C}$ with $E^{(\mathcal{C})}_{\mathrm{SRG}}(J \leq \frac{7}{2}) = 40$ and $E^{(\mathcal{C})}_{\mathrm{SRG}}(J \geq \frac{13}{2}) = 34$, and $\mathcal{D}$ with $E^{(\mathcal{D})}_{\mathrm{SRG}}(J \leq \frac{5}{2}) = 40$ and $E^{(\mathcal{D})}_{\mathrm{SRG}}(J \geq \frac{9}{2}) = 36$, which probe the large-$J$ part of the 3N SRG model space that is vital for heavier systems. In Fig. 2(b) we show the deviation of the CCSD ground-state energies for ramps $\mathcal{C}$ and $\mathcal{D}$ from the largest ramp $\mathcal{B}$. These deviations are below 50 keV per nucleon even for the heaviest nuclei, which confirms convergence with respect to the SRG model-space size, and establishes ramp $\mathcal{B}$ as the standard used in the following. We have also confirmed that the truncation in the low-J part of the model space introduced only negligible errors.

5. CC convergence and triples correction

Soft interactions allow for reasonably well converged CC calculations at $e_{\mathrm{max}} = 12$, as is apparent from Fig. 3, where we present ground-state energies from CCSD, ΛCCSD(T) [4,34,35], and CR-CC(2,3) [31–33,38]. Both triples-correction methods are highly sophisticated and we note that the former can be obtained as an approximation to the latter [27]. We observe noticeable differ-

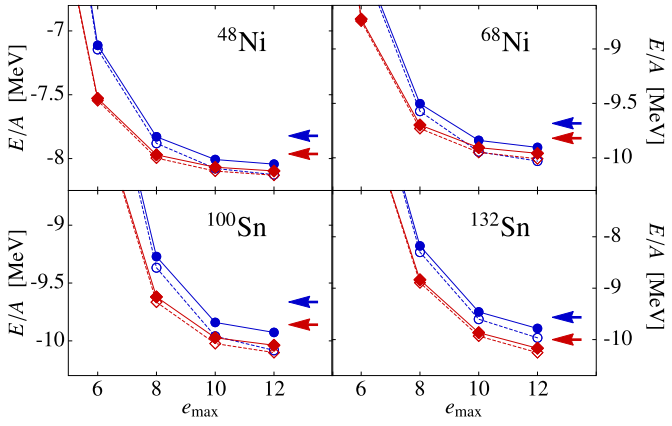

Fig. 3. (Color online.) Convergence of CR-CC(2,3) (full symbols) and ΛCCSD(T) (open symbols) ground-state energies for the $NN+3N$-full Hamiltonian at $\alpha = 0.04$ fm^4 (blue circles) and 0.08 fm^4 (red diamonds), and with $E_{3\,\max} = 14$ and $\hbar\Omega = 24$ MeV. Also shown are CCSD ground-state energies (arrows) from $e_{\max} = 12$ model spaces, where the upper (blue) arrows correspond to $\alpha = 0.04$ fm^4.

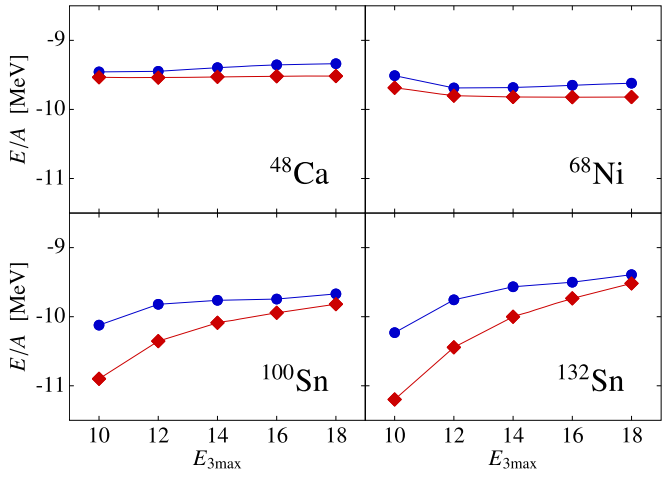

Fig. 4. (Color online.) Convergence of CCSD ground-state energies from $e_{\max} = 12$ CC model spaces, for the $NN+3N$-full Hamiltonian at $\alpha = 0.04$ fm^4 (blue circles) and 0.08 fm^4 (red diamonds) with respect to $E_{3\,\max}$. Other parameters of the Hamiltonian as in Fig. 3.

ences for the $\alpha = 0.04$ fm^4 interaction, where the magnitude of the triples correction itself is larger than for $\alpha = 0.08$ fm^4, with the ΛCCSD(T) results lying below their CR-CC(2,3) counterparts. This is consistent with findings from quantum chemistry, where ΛCCSD(T) tends to overestimate the exact triples correction [39]. In the following, we use the size of the CR-CC(2,3) triples correction to estimate the rate of convergence of the cluster expansion.

6. Normal-ordering procedure

Because full matrix element sets with $E_{3\,\max} \approx 16$ become inconveniently large [13], we follow a procedure that avoids storage of full sets of $E_{3\,\max} > 14$ matrix elements. In a first step we perform an HF calculation including the complete $3N$ interaction up to $E_{3\,\max} = 14$ and use the HF ground state as reference for the normal-ordering of the $3N$ interaction with the larger $E_{3\,\max}$, where we selectively compute the subset of JT-coupled $3N$ matrix elements [13] directly entering the normal-ordering. Using the NO2B matrix elements we perform another HF calculation to obtain a reference state including the large-$E_{3\,\max}$ information. This process can be iterated until consistency is achieved, but a single iteration is typically sufficient. In Fig. 4 we present CCSD ground-state energies of various nuclei using $E_{3\,\max} = 10$ up to 18. For the lighter nuclei ^{48}Ca and ^{68}Ni, convergence is reached around $E_{3\,\max} = 14$. The situation changes for the heavier nuclei ^{100}Sn and ^{132}Sn, where the large values of $E_{3\,\max}$ are in fact necessary to achieve convergence.

The NO2B approximation is crucial since it allows to handle large values of $E_{3\,\max}$. However, earlier works show that for soft interactions contributions of the residual normal-ordered $3N$ interaction can become comparable to the triples correction [27,36]. Most of these contributions stem from CCSD, while the residual $3N$ interactions may be neglected in the triples correction [27]. Therefore, in the following we explicitly include the residual $3N$ interaction up to $E_{3\,\max} = 12$ when we solve the CCSD equations [26,36], and use the NO2B matrix elements to cover the $3N$ contributions up to $E_{3\,\max} = 18$. Particularly for the Ca and Ni isotopes, this practically eliminates the error of the NO2B approximation [27,36]. The remaining largest sources of uncertainty are given by the convergence with respect to model space, the $E_{3\,\max}$ cut and the cluster truncation. An overall analysis of these uncertainties suggests that for a given Hamiltonian at fixed α, we obtain the energies with an accuracy of approximately 2% for Ni, and 2–4% for Sn isotopes. We estimate the level of convergence with respect to model space from the difference of CCSD results at $e_{\max} = 12$ and 14. For ^{100}Sn and $\alpha = 0.04$ fm^4, for example, this results in an uncertainty of about 0.9%. Similarly, the level of convergence with respect to $E_{3\,\max}$ is based on the $E_{3\,\max} = 16$ and 18 data, which for ^{100}Sn and $\alpha = 0.04$ fm^4 leads to an uncertainty estimate of about 0.6%. Finally, the convergence with respect to the cluster truncation is estimated from the size of the triples correction, which is about 2.7% for ^{100}Sn and $\alpha = 0.04$ fm^4 and about 1.8% for $\alpha = 0.08$ fm^4, resulting in a total error of about 2.9% for $\alpha = 0.04$ fm^4 and 1.9% for $\alpha = 0.08$ fm^4. In all of our calculations, the error is dominated by the cluster truncation and we note that due to the fast convergence of the cluster expansion our employed error estimate is very conservative.

7. Heavy nuclei from chiral Hamiltonians

The developments discussed above enable us to extend the range of accurate *ab initio* calculations into the regime of heavy nuclei. In Fig. 5 we present ground-state energies of closed subshell nuclei ranging from ^{16}O to ^{132}Sn for SRG-evolved chiral Hamiltonians with $E_{3\,\max} = 18$ and for the two resolution scales $\alpha = 0.04$ fm^4 and $\alpha = 0.08$ fm^4 used to study the α-dependence. In panels (a) and (c) we show ground-state energies obtained from CR-CC(2,3) in comparison to experiment, in panels (b) and (d) we depict the size of the triples correction beyond CCSD.

First we consider the $NN+3N$-induced results shown in Fig. 5(a). With increasing mass number, we observe a significant increase in the α-dependence indicating growing contributions of SRG-induced $4N$ (and multi-nucleon) interactions resulting from the initial NN interaction. To confirm this trend, we show results starting from the optimized chiral NN interaction N^{2}LO$_{\rm opt}$ presented in Ref. [40] in addition to the chiral NN interaction at N^{3}LO of Ref. [19] used in all other calculations. Previous investigations have shown that when starting from a chiral NN Hamiltonian, induced $4N$ contributions are small for p- or lower sd-shell nuclei [8,13,22] – this is confirmed within the truncation uncertainties by the present calculations. However, the effect of the omitted $4N$ contributions is amplified when going to heavier nuclei and the α-dependence indicates that these induced $4N$ interactions are attractive.

If we add the initial $3N$ interaction to the chiral NN interaction at N^{3}LO the picture changes. The α-dependence of the $NN+3N$-full Hamiltonian is significantly reduced compared to the

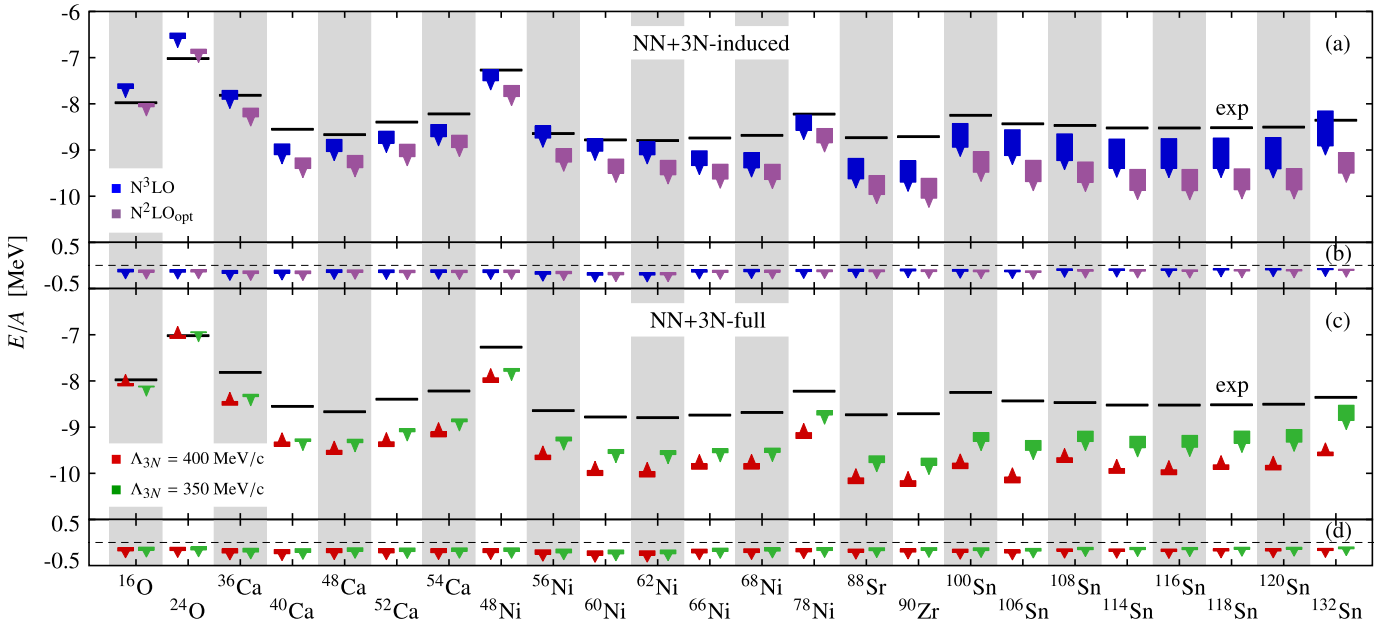

Fig. 5. (Color online.) Ground-state energies from CR-CC(2,3) for (a) the $NN+3N$-induced Hamiltonian starting from the N^{3}LO and N^{2}LO-optimized NN interaction and (c) the $NN+3N$-full Hamiltonian with $\Lambda_{3N}=400$ MeV/c and $\Lambda_{3N}=350$ MeV/c. The boxes represent the spread of the results from $\alpha=0.04$ fm^4 to $\alpha=0.08$ fm^4, and the tip points into the direction of smaller values of α. Also shown are the contributions of the CR-CC(2,3) triples correction to the (b) $NN+3N$-induced and (d) $NN+3N$-full results. All results employ $\hbar\Omega=24$ MeV and $3N$ interactions with $E_{3\,\max}=18$ in NO2B approximation and full inclusion of the $3N$ interaction in CCSD up to $E_{3\,\max}=12$. Black bars denote energies taken from [37,40].

$NN+3N$-induced results, as seen in Fig. 5(c). In addition to the local $3N$ interaction at N^{2}LO with initial cutoff $\Lambda_{3N}=400$ MeV/c, we employ a second cutoff $\Lambda_{3N}=350$ MeV/c for comparison [13]. Our previous studies have shown that for both cutoffs, the induced $4N$ interaction is small up into the sd-shell [8,13]. For heavier nuclei, Fig. 5(c) reveals that the α-dependence of the ground-state energies remains small for $\Lambda_{3N}=400$ MeV/c up to the heaviest nuclei. Thus, the attractive induced $4N$ contributions that originate from the initial NN interaction are canceled by additional repulsive $4N$ contributions originating from the initial chiral $3N$ interaction. By reducing the initial $3N$ cutoff to $\Lambda_{3N}=350$ MeV/c, the repulsive $4N$ component resulting for the initial $3N$ interaction is weakened [13] and the attractive induced $4N$ from the initial NN prevails, leading to an increased α-dependence indicating an attractive net $4N$ contribution. All of these effects are larger than the truncation uncertainties of the calculations, such as the cluster truncation, as is evident by the comparatively small triples contributions shown in Fig. 5(b) and (d).

Because we cannot include the induced $4N$ interactions, we take advantage of the cancellation of these terms for the $NN+3N$-full Hamiltonian with $\Lambda_{3N}=400$ MeV/c in order to compare the energies to experiment. Throughout the different isotopic chains starting from Ca, the experimental pattern of the binding energies is reproduced up to a constant shift of the order of 1 MeV per nucleon. The stability and qualitative agreement of the these results over an unprecedented mass range is remarkable, given the fact that the Hamiltonian was determined in the few-body sector alone.

When considering the quantitative deviations, one has to consider the consistent chiral $3N$ interaction at N^{3}LO, and the initial $4N$ interaction. In particular for heavier nuclei, the contribution of the leading-order $4N$ interaction might be sizable. Another important future aspect is the study of other observables, such as charge radii. In the present calculations the charge radii of the HF reference states are systematically smaller than experiment and the discrepancy increases with mass. For ^{16}O, ^{40}Ca, ^{88}Sr, and ^{120}Sn the calculated charge radii are 0.3 fm, 0.5 fm, 0.7 fm, and 1.0 fm too small [41]. These deviations are larger than the expected effects of beyond-HF correlations and consistent SRG-evolutions of the radii. This discrepancy will remain a challenge for future studies of medium-mass and heavy nuclei with chiral Hamiltonians.

8. Conclusions

In this Letter we have presented the first *ab initio* calculations for heavy nuclei using SRG-evolved chiral interactions. We have identified and eliminated a number of technical hurdles, e.g., regarding the SRG model space, that have inhibited state-of-the-art medium-mass approaches to address heavy nuclei. As a result, many-body calculations up to ^{132}Sn are now possible with controlled uncertainties on the order of approximately 2% for Ni, and 2–4% for Sn isotopes. The qualitative agreement of ground-state energies for nuclei ranging from ^{16}O to ^{132}Sn obtained in a single theoretical framework demonstrates the potential of *ab initio* approaches based on chiral Hamiltonians. This is a first direct validation of chiral Hamiltonians in the regime of heavy nuclei using *ab initio* techniques. Future studies will have to involve consistent chiral Hamiltonians at N^{3}LO considering initial and SRG-induced $4N$ interactions and provide an exploration of other observables.

Acknowledgements

We thank Piotr Piecuch for helpful discussions and Petr Navrátil for providing us with the ManyEff code [42]. Supported by the Deutsche Forschungsgemeinschaft through contract SFB 634, by the Helmholtz International Center for FAIR (HIC for FAIR) within the LOEWE program of the State of Hesse, and the BMBF through contract 06DA7047I. Numerical calculations have been performed at the computing center of the TU Darmstadt (lichtenberg), at the Jülich Supercomputing Centre (juropa), at the LOEWE-CSC Frankfurt, and at the National Energy Research Scientific Computing Center supported by the Office of Science of the U.S. Department of Energy under Contract No. DE-AC02-05CH11231.

References

[1] R. Machleidt, D.R. Entem, Phys. Rep. 503 (2011) 1.
[2] E. Epelbaum, H.-W. Hammer, U.-G. Meißner, Rev. Mod. Phys. 81 (2009) 1773.
[3] S.K. Bogner, R.J. Furnstahl, A. Schwenk, Prog. Part. Nucl. Phys. 65 (2010) 94, arXiv:0912.3688.
[4] G. Hagen, T. Papenbrock, D.J. Dean, M. Hjorth-Jensen, Phys. Rev. C 82 (2010) 034330.
[5] E. Epelbaum, H. Krebs, D. Lee, U.-G. Meißner, Eur. Phys. J. A 45 (2010) 335.
[6] G. Hagen, M. Hjorth-Jensen, G.R. Jansen, R. Machleidt, T. Papenbrock, Phys. Rev. Lett. 108 (2012) 242501.
[7] S. Bacca, N. Barnea, G. Hagen, G. Orlandini, T. Papenbrock, Phys. Rev. Lett. 111 (2013) 122502.
[8] H. Hergert, S. Binder, A. Calci, J. Langhammer, R. Roth, Phys. Rev. Lett. 110 (2013) 242501.
[9] B.R. Barrett, P. Navrátil, J.P. Vary, Prog. Part. Nucl. Phys. 69 (2013) 131, ISSN 0146-6410.
[10] T. Lähde, E. Epelbaum, H. Krebs, D. Lee, U. Meißner, G. Rupak, arXiv:1311.0477 [nucl-th], 2013.
[11] G. Hupin, J. Langhammer, P. Navrátil, S. Quaglioni, A. Calci, R. Roth, Phys. Rev. C 88 (2013) 054622.
[12] R. Roth, Phys. Rev. C 79 (2009) 064324.
[13] R. Roth, A. Calci, J. Langhammer, S. Binder, arXiv:1311.3563 [nucl-th], 2013.
[14] V. Somà, T. Duguet, C. Barbieri, Phys. Rev. C 84 (2011) 064317.
[15] A. Cipollone, C. Barbieri, P. Navrátil, Phys. Rev. Lett. 111 (2013) 062501.
[16] V. Somà, A. Cippolone, C. Barbieri, P. Navrátil, T. Duguet, arXiv:1312.2068 [nucl-th], 2013.
[17] K. Tsukiyama, S.K. Bogner, A. Schwenk, Phys. Rev. Lett. 106 (2011) 222502.
[18] H. Hergert, S.K. Bogner, S. Binder, A. Calci, J. Langhammer, R. Roth, A. Schwenk, Phys. Rev. C 87 (2013) 034307.
[19] D.R. Entem, R. Machleidt, Phys. Rev. C 68 (2003) 041001(R).
[20] P. Navrátil, Few-Body Syst. 41 (2007) 117.
[21] R. Roth, J. Langhammer, A. Calci, S. Binder, P. Navrátil, Phys. Rev. Lett. 107 (2011) 072501.
[22] R. Roth, S. Binder, K. Vobig, A. Calci, J. Langhammer, P. Navrátil, Phys. Rev. Lett. 109 (2012) 052501.
[23] S.K. Bogner, R.J. Furnstahl, R.J. Perry, Phys. Rev. C 75 (2007) 061001(R).
[24] E.D. Jurgenson, P. Navrátil, R.J. Furnstahl, Phys. Rev. Lett. 103 (2009) 082501.
[25] R. Roth, T. Neff, H. Feldmeier, Prog. Part. Nucl. Phys. 65 (2010) 50.
[26] G. Hagen, T. Papenbrock, D.J. Dean, A. Schwenk, A. Nogga, M. Włoch, P. Piecuch, Phys. Rev. C 76 (2007) 034302.
[27] S. Binder, P. Piecuch, A. Calci, J. Langhammer, P. Navrátil, R. Roth, Phys. Rev. C 88 (2013) 054319.
[28] M. Włoch, D. Dean, J. Gour, M. Hjorth-Jensen, K. Kowalski, T. Papenbrock, P. Piecuch, Phys. Rev. Lett. 94 (2005) 212501.
[29] G. Hagen, T. Papenbrock, D.J. Dean, M. Hjorth-Jensen, Phys. Rev. Lett. 101 (2008) 092502.
[30] G.D. Purvis III, R.J. Bartlett, J. Chem. Phys. 76 (1982) 1910.
[31] P. Piecuch, M. Włoch, J. Chem. Phys. 123 (2005) 224105.
[32] P. Piecuch, J.R. Gour, M. Włoch, Int. J. Quant. Chem. 109 (2009) 3268.
[33] S. Binder, P. Piecuch, in preparation.
[34] A.G. Taube, R.J. Bartlett, J. Chem. Phys. 128 (2008) 044110.
[35] A.G. Taube, R.J. Bartlett, J. Chem. Phys. 128 (2008) 044111.
[36] S. Binder, J. Langhammer, A. Calci, P. Navrátil, R. Roth, Phys. Rev. C 87 (2013) 021303(R).
[37] M. Wang, G. Audi, A. Wapstra, F. Kondev, M. MacCormick, X. Xu, B. Pfeiffer, Chin. Phys. C 36 (2012) 1603.
[38] R. Roth, J.R. Gour, P. Piecuch, Phys. Rev. C 79 (2009) 054325.
[39] A.G. Taube, Mol. Phys. 108 (2010) 2951.
[40] A. Ekström, G. Baardsen, C. Forssén, G. Hagen, M. Hjorth-Jensen, G.R. Jansen, R. Machleidt, W. Nazarewicz, T. Papenbrock, J. Sarich, et al., Phys. Rev. Lett. 110 (2013) 192502.
[41] H.D. Vries, C.D. Jager, C.D. Vries, At. Data Nucl. Data Tables 36 (1987) 495.
[42] P. Navrátil, G.P. Kamuntavicius, B.R. Barrett, Phys. Rev. C 61 (2000) 044001.